

# Effect of Humidity on Time- and Velocity-Dependent Friction in Rocks

JAMES H. DIETERICH AND GERALD CONRAD

*U.S. Geological Survey*

Friction experiments were conducted utilizing samples tested in a humid atmosphere (ambient laboratory humidity or argon bubbled through water) and samples that were carefully dried and tested in an atmosphere of very dry argon ( $H_2O < 1$  ppm). Dry surfaces consistently yield a friction coefficient of 0.85 to 1.00 compared with 0.55 to 0.65 for the tests in a humid environment. Time-dependent increases in the friction coefficient and large-scale stick-slip instability are characteristic of surfaces exposed to atmospheric water, but they are eliminated with careful drying. Direct dependence of frictional strength on slip speed persists under both dry and humid conditions.

## INTRODUCTION

Traces of moisture facilitate many well-known physical and chemical processes in which the moisture is neither visually nor inferentially obvious. An example that is particularly relevant to geophysics is the familiar weakening effects of water on silicates. The purpose of the experiments described here was to look for possible effects of humidity or adsorbed water on the frictional properties of rocks. In particular, our aim was to determine if time- and velocity-dependent friction phenomena originate from the chemical effects of water. These time- and velocity-dependent effects apparently underlie many frictionally controlled processes including stick-slip instability, preinstability stable sliding, and oscillatory slip. Improved understanding of these effects may yield insights for understanding the processes accompanying earthquake instability on crustal faults which are thought to be frictional in nature. *Dieterich* [1978] proposed that unstable slip in rocks requires the presence of trace amounts of water and that slip under truly dry conditions should be stable, a prediction that is tested and partially confirmed by this study.

This study is based on comparisons between rock friction tests conducted under humid conditions and tests in which attempts were made to remove all traces of free or adsorbed water from the samples and from the testing environment.

## FRICION EFFECTS OBSERVED UNDER HUMID CONDITIONS

Rock friction experiments conducted under conditions of atmospheric humidity show a variety of time-, velocity-, and displacement-dependent effects [*Dieterich*, 1972, 1978, 1979, 1981; *Scholz et al.*, 1972; *Ruina*, 1983; *Higgs and Logan*, 1981]. Although the published rock friction studies report a range of results, some apparently contradictory, *Dieterich* [1979, 1981] proposed that most, if not all, of the observations can be explained as arising from three processes that operate simultaneously during slip. The proposed mechanisms include two rate-dependent processes controlling the strength of load-bearing contacts between the surfaces and a process of continuous changes in the population of contacts due to displacement of the surfaces. These processes are not well understood, but they are amenable to quantification in constitutive laws and measurement in laboratory experiments. Constitutive laws of the general type proposed by *Dieterich* [1979, 1981]

appear to represent adequately these processes and reproduce the range of phenomena observed in experiments. The mechanisms appear to be valid for clean, gouge-free sliding surfaces and for surfaces separated by a layer of artificial fault gouge.

The first process is an increase in the strength of the load-supporting contacts between the surfaces with age of the contacts. This process is most clearly evident in experiments in which the sliding surfaces are held in nominally stationary contact under shear stress (to prevent disruption of the points of contact) for varying intervals of time prior to slip. Experimental data show that the coefficient of friction  $\mu$  (ratio of shear to normal stress) increases with the logarithm of the age of contacts (Figure 1). The process is apparently caused by creep that increases the real area of the load-bearing contacts [*Dieterich*, 1972, 1978; *Scholz et al.*, 1972]. The creep may increase the shear strength (friction) by increasing the true area of adhesive contact or by increased penetration depth of asperities that increase the ploughing component of the frictional force. In most situations it may be inferred that the latter mechanism is probably less important than the former [*Dieterich*, 1978].

Under conditions of atmospheric humidity, creep at points of contact (resulting in increases of the area of contact with the logarithm of the time of contact) appears to be a general characteristic of nonmetallic solids including rock-forming minerals. Microindentation experiments have definitively established these effects for a wide class of materials [*Westbrook and Jorgensen*, 1965, 1968; *Walker and Demer*, 1964; *Scholz and Engelder*, 1976; *Evans and Goetze*, 1979]. Indentation creep effects at room temperature have been identified by *Westwood et al.* [1967] as belonging to a broad class of chemomechanical surface weakening effects. Area of contact under an indenter increases because of creep (or equivalently time-dependent reductions of surface hardness) that is assisted by the presence of mechanically active chemical agents. Indentation experiments conducted in various chemical environments show varying amounts of indentation creep. Under extremely dry conditions the indentation creep effect has been found to be greatly reduced or entirely eliminated [*Westbrook and Jorgensen*, 1965]. Hence friction tests conducted on surfaces that do not have surface water are expected not to show the effects illustrated by Figure 1.

A second process is slip-induced disruption of the load-bearing contacts. During slip it is evident that points on one surface in actual contact with the opposite surface must continuously change with displacement. The process of contact formation and change is not well studied but may involve both the sliding of protuberances on one surface (asperities)

This paper is not subject to U.S. copyright. Published in 1984 by the American Geophysical Union.

Paper number 3B1727.

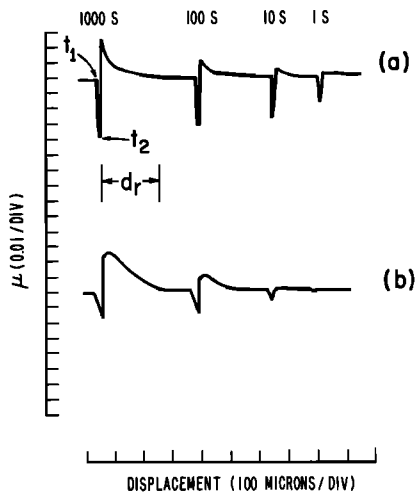


Fig. 1. Coefficient of friction  $\mu$  versus displacement showing time and displacement dependence of frictional strength for Westerly granite with 2 mm of gouge on sliding surfaces and at 10.0-MPa normal stress. (a) Experiment and (b) theoretical prediction using the constitutive model (modified from Dieterich [1981]). In these tests, vertical driving ram is held stationary beginning at time  $t_1$ . Motion of the ram resumes at  $t_2$ . Relaxation during hold is caused by continuing slip of the surface. Hold times ( $t_1 - t_2$ ) are indicated above the curves. The parameter  $d_r$  is the displacement at which  $\mu$  returns to the residual sliding value.

across the opposite surface and the creation of contacts as two irregularities on opposite surfaces are brought together followed by loss of contact by destruction of the irregularities or by physical separation. In any case, it is clear that the average time of contact between two opposite points on the sliding surfaces must depend inversely on slip speed. Therefore it has been proposed [Dieterich, 1978] that the area of contact between sliding surfaces depends inversely on slip speed. Consequently, in the absence of other effects, the first two processes (increasing strength with age and inverse dependence of contact age on velocity) tend to produce an overall weakening of the frictional strength with increased velocity. Similarly, sliding displacement of a surface that has been stationary for an interval of time will undergo slip weakening as the average age of the contacts evolves from the initial hold time to a smaller time of contact characteristic of the sliding velocity. The displacement weakening following the friction peaks in Figure 1 is explained as resulting from these two mechanisms. The sliding displacement required to change the frictional strength (parameter  $d_r$  in Figure 1) is interpreted to be the displacement required to completely change the age of the population of contacts from the initial hold time to the smaller time characteristic of the sliding velocity. The interpretation that  $d_r$  is the average displacement needed to change the population of points in contact is supported by correlation of  $d_r$  with surface roughness and gouge particle size [Dieterich, 1981]. The parameter  $d_r$  increases with surface roughness and with grain size of artificial fault gouge placed between the sliding surfaces.

It has been demonstrated that displacement weakening of the type shown in Figure 1 can lead to stick-slip instability [Dieterich, 1978]. Hence if the time-dependent strengthening of the contacts is the result of water-assisted surface weakening, then displacement weakening and consequently stick slip should be reduced or eliminated in dry experiments.

The third process is an inferred direct dependence of the

shear strength of the load-bearing contacts on the rate of shear displacement of the sliding surfaces. For an apparently fixed area of contact, an increase in slip rate results in an increase in friction. Equivalently, load-bearing contacts that permit rapid slip at elevated stress are capable of creeping slip at reduced loads. It is important to note that this rate dependence in shear produces an effect that is distinct from and opposite in sign to the velocity dependence arising from interaction of the first two processes. The third process is most evident when the slip velocity is rapidly changed (Figure 2). Because of this third effect a change in slip velocity produces an immediate change in frictional resistance that is of the same sign as the change in velocity. However, as slip progresses at the new velocity, the age of the load-bearing contacts begins to evolve to a new population with an average age that is characteristic of the new velocity. As this takes effect, the rate dependence arising from the first two processes becomes increasingly important and acts in the opposite sense to the initial velocity dependence. At displacements exceeding  $d_r$ , the net change in friction for a change in velocity is determined by all three of these processes. Net positive and negative dependence of friction on slip rate have been observed.

The third process is not well understood, but by inference it appears to be related to the process of shear failure of the load-bearing contacts as the surfaces slide. The processes by which the points of contact support applied shear loads then yield to produce slip may involve slip and pulling apart of adhesive junctions, localized plastic yielding of irregularities, and brittle failure of irregularities. The observed direct dependence of this process on velocity is consistent with failure of contacts in shear aided by water weakening by either enhanced crack growth or by creep.

#### APPARATUS AND PROCEDURES FOR DRY EXPERIMENTS

Microindentation experiments, cited above, suggest that very small amounts of adsorbed water can have a profound effect on the mechanical properties of silicate surfaces. Therefore principal considerations in the design of experiments were to find an effective means for drying the samples and to isolate the dried surfaces from atmospheric humidity at all subsequent stages of the experiment. The approach adopted for

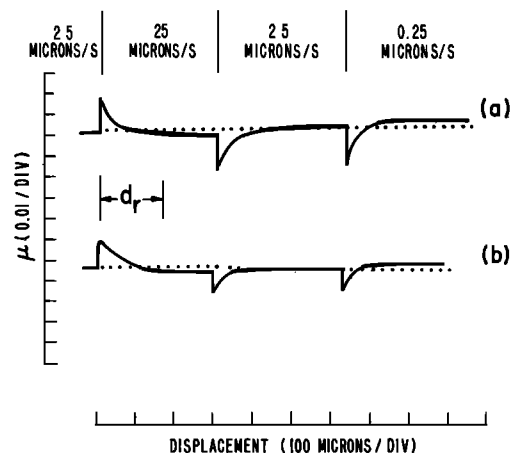


Fig. 2. Velocity dependence of frictional strength for Westerly granite with 2 mm of gouge on the sliding surfaces and at 10.0-MPa normal stress. (a) Experiment and (b) theoretical prediction using the constitutive model (modified from Dieterich [1981]).

these experiments was to conduct the drying and friction testing in a single vessel that was isolated from the atmosphere at all times. Drying is accomplished by heating, usually to 300°C in an atmosphere of very dry argon ( $H_2O < 1$  ppm) for approximately 16 hours. The argon supply line was purged of water by heating with a blow torch while dry argon was flushed through the system. Considerable variability in results was encountered especially in the early tests. We ascribed this variability to incomplete drying and to contamination. As a result, a number of refinements to this general procedure evolved as experimental difficulties were encountered. Ultrasonic cleaning of the sliding surfaces (with detergent solution, followed by water and acetone rinses) to remove grinding debris trapped in surface irregularities and cleaning of the vessel used to isolate the sample from the atmosphere resulted in significantly reduced experimental variability. These steps were used for all tests reported below. To facilitate cleaning and to reduce possible contamination of the sample with water or other volatiles released from the walls of the chamber, all surfaces of the chamber were plated with nickel followed by gold.

The sample configuration consists of the three-block direct shear arrangement described previously [Dieterich, 1972]. Figure 3 illustrates the sample assembly and isolation chamber. The sliding surfaces have nominal dimensions of 50 mm  $\times$  50 mm. Clamps are used to fasten samples to the steel pistons. The horizontal pistons which apply normal stress to the sliding surfaces slide through slightly oversized holes in the chamber walls. A small positive pressure of argon is maintained at all times to prevent atmospheric contaminants from entering the chamber through these openings and to provide a continuous flush of dry argon through the chamber. The vertical ram which applies the shear stress to the sliding surfaces is attached to the chamber by means of a nickel diaphragm 0.13 mm thick. The diaphragm permits approximately 1 cm of sliding displacement. During the drying phase, when the sample is heated using an internal heater, the pistons are held in a partially retracted position to expose the sliding surfaces. During the cooling phase the pistons are advanced to bring the sliding surfaces into contact. In general, high argon flow rates were used during the drying phase (0.4–0.5 l/min) and lower argon flow rates (0.2 l/min) were used during cooling and friction

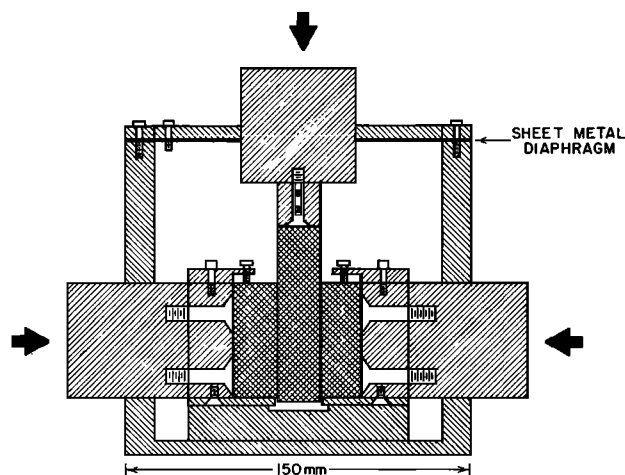


Fig. 3. Sample assembly for dry and control experiments. Not shown are internal heating element, thermocouple access, and inlet port for dry or humid argon.

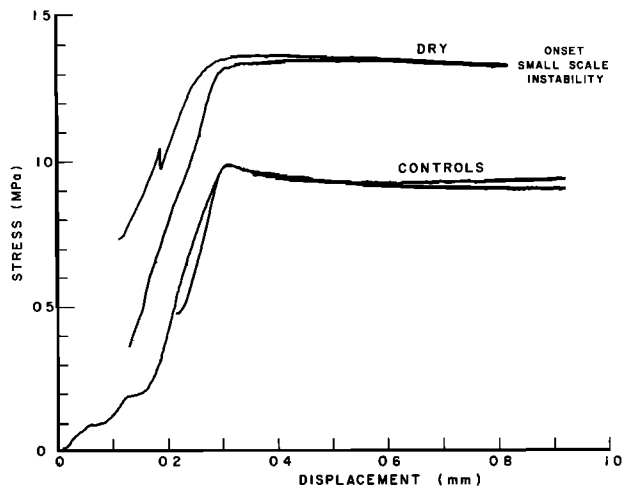


Fig. 4. Control and dry tests with Eureka quartzite at servo-control constant slip velocity of 1.0  $\mu\text{m/s}$ . Normal stress is 1.7 MPa.

testing. The lower flow rates were used because it was suspected that over long intervals of time the cool dry surfaces might become recontaminated by the trace amounts of water carried in the argon.

Exploratory experiments were conducted with Westerly granite, single-crystal quartz, and Eureka quartzite. The quartzite is fine-grained, dense, quartz cemented and with few impurities. Each material yielded similar results that correlated with humidity. Because the quartzite was compositionally simpler than the granite and is easier to work with than the single-crystal quartz, it was chosen for the more extensive tests reported here. Sliding surfaces were prepared by surface grinding to insure flatness and parallelism followed by hand lapping with 240 mesh silicon carbide abrasive to produce a uniform and reproducible roughness.

It was inferred from exploratory experiments that humidity trapped in the interior of the specimen gradually recontaminated the sliding surfaces during an experiment. Higher stresses apparently accelerated the recontamination by opening more pathways to conduct trapped moisture from the interior to the sliding surfaces. As a result of this, all tests were conducted at a low normal stress of 1.7 MPa. This low normal stress is not considered detrimental because previous experiments under humid conditions establish that the rate-dependent processes of interest for this study operate over a wide range of normal stresses including the low stresses employed here (e.g., Dieterich [1972] found similar time-dependent increases in the coefficient of friction at all normal stresses examined from 2.0 MPa to 85 MPa).

Because the range friction phenomena observed under humid conditions apparently involve competing processes, no single type of experimental test has been found that adequately isolates all of the relevant processes. Therefore to evaluate the effects of drying, three types of tests were conducted on dried samples and on samples exposed to a humid environment: (1) constant velocity sliding experiments, (2) slide and hold tests of the type shown in Figure 1, and (3) velocity stepping tests of the type illustrated in Figure 2.

In most tests, unless otherwise specified, slip velocity and displacement were controlled using a high-speed hydraulic servo-control system. This system employs displacement measurements from a transducer spanning the sample assembly as the feedback signal that follows preprogrammed

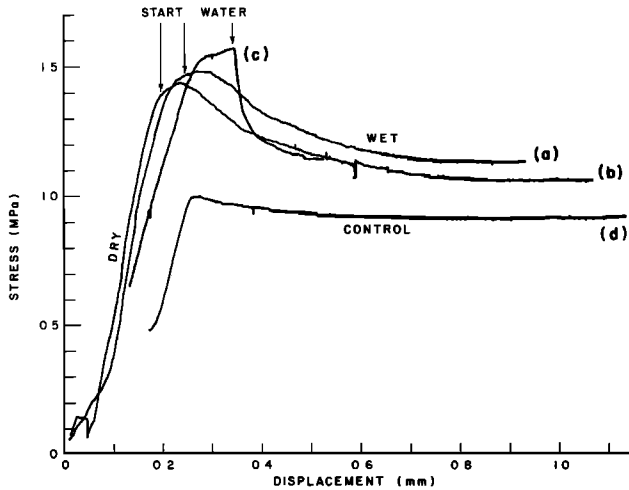


Fig. 5. Effect of admitting humid argon to a dry sample of Eureka quartzite after sliding has commenced. See text for explanation of Figures 5a–5c. For comparison, Figure 5d is one of the air-dried control experiments shown in Figure 4. Normal stress is 1.7 MPa. Slip velocity is  $1.0 \mu\text{m/s}$ .

displacement versus time signals provided by a laboratory computer. The measured displacements and the displacements indicated in the following figures are the sum of slip and elastic shortening of the sample assembly. Additional details of the system are outlined in the work of Dieterich [1981]. This servo-control system has sufficiently high effective mechanical stiffness and rapid response rates to inhibit stick-slip instability at these normal stresses for humid conditions. For some tests a manually set needle valve was used to provide a constant rate of supply of hydraulic oil to the driving ram instead of employing servo-control. Use of the needle valve to control loading rates in place of the servo-controlled system greatly reduces the effective mechanical stiffness of the system that loads the sample assembly permitting stick-slip instability under humid conditions.

## RESULTS

Figure 4 shows results of tests at a servo-controlled constant slip velocity of  $1.0 \mu\text{m/s}$ . The curves labeled "dry" were obtained using samples of quartzite prepared and dried following the standard procedure described above. The control experiments were conducted in the drying chamber using identical procedures, except the samples were air dried only, without heating or dry argon flow. The air-dried control experiments which had access to atmospheric humidity at all times consistently yielded a coefficient of friction that stabilizes at 0.55 to 0.65, a range of values that is typical for air-dried or water-saturated silicates. The samples dried in argon yield unusually high coefficients of friction in the range 0.85 to 1.00.

Tests in which the samples were prepared and dried using the standard procedure followed by admittance of humid argon to the testing chamber after the sliding at the high friction levels had commenced are given in Figure 5. For the "wet" tests the argon was bubbled through a water bath prior to entering the test chamber. We assume the relative humidity was approximately 100%. In each of these tests the frictional strength rapidly begins to drop after the humid argon enters the testing chamber. Figures 5a and 5b pertain to samples prepared and dried using the standard procedure. In Figure 5c

a grid of 1-mm-deep grooves was cut into one of each pair of sliding surfaces to facilitate access of the humid argon to the sliding surfaces. The grooves are spaced 1 cm and are oriented parallel and perpendicular to the slip direction. Control tests indicate that the surface grooves do not alter frictional response under conditions of atmospheric humidity.

To examine the effect of drying on time dependence of friction, slide and hold tests were conducted. In these tests, sliding was maintained at a constant velocity ( $5\text{--}10 \mu\text{m/s}$ ) until the friction stabilized at a reasonably uniform level (this usually occurred following a few millimeters of displacement), then the driving ram was held stationary for specified intervals of time followed by slip at constant velocity and initiation of another hold cycle, etc. The experiments in Figure 6 illustrate the range of effects observed in the dry and control experiments. The dry tests do not show the characteristic time-dependent strengthening effect seen in the tests with atmospheric humidity. During the hold intervals while the displacements were held constant, the shear stress applied to the sample relaxed with time. Earlier studies [Dieterich, 1981] confirmed by careful examination of the shear displacements records from these tests indicate that this stress relaxation is caused by creep of the sliding surfaces (i.e., continued slow slip). The creep persisted in the dry tests. It is of interest that the experiments appear to follow a consistent pattern of greater stress relaxation under the dry conditions than under the humid conditions. Exposure of the dried samples to humid argon always restored the time-dependent strengthening effect.

In tests without high-speed servo-control of displacement rates, the time-dependent strengthening effect for humid samples can lead to stick-slip instability (Figure 7). Stick slip of this type did not occur in similar dry experiments. In dry experiments that did not have high-speed servo-control, particularly with exploratory tests at higher normal stresses the effect of admitting humid argon to the test chamber could be dramatic: Quiet stable slip would be replaced by loud stick-slip sliding within a few seconds of exposure of the sample to the humid atmosphere.

Results of representative velocity stepping experiments for dry and humid conditions are given by Figure 8. The control experiments (air dried and tested in humid air) are consistent with previously reported results under humid conditions. A velocity increase leads to an immediate increase in sliding friction followed by displacement-dependent decay in strength to a residual strength slightly less than the sliding friction at

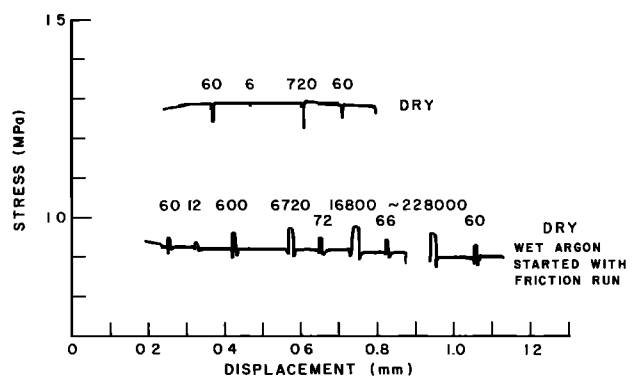


Fig. 6. Time dependence tests for dry samples of Eureka quartzite and for samples reexposed to humid argon during test. Driving velocity between hold intervals is  $1.0 \mu\text{m/s}$ . Hold intervals, in seconds, is given above the curves. Normal stress is 1.7 MPa.

the previous velocity. In contrast, the dry samples showed the immediate jump of strength when velocity was changed, but the opposing displacement-dependent change in strength was either eliminated or significantly reduced (in comparison with the humid tests). As a result, the net dependence of frictional strength on slip velocity for the dry tests is of opposite sign of that for the humid tests. In the dry tests, an increase in slip velocity resulted in a net increase in sliding resistance. Degradation of the net positive velocity dependence at large displacements often occurred and may have been caused by recontamination of the surfaces by water trapped in the sample.

In some dry experiments an unusual instability process with previously unreported characteristics was observed, particularly if large sliding displacements were quickly reached (Figure 9). The instabilities, which could not be inhibited by our high-speed servo-control system, were accompanied by very small displacements (calculated from the stress drops to be 2–5  $\mu\text{m}$ ) and produced a sound best described as a quiet click from the sample assembly. By comparison the usual stick-slip instability seen under humid conditions can be inhibited by high-speed servo-control. Stick slip in the low stiffness, nonservo-controlled system is characterized by a noisy bang and by large displacements (20–60  $\mu\text{m}$ ) during the instability. These characteristics indicate that the instabilities in the dry experiments are localized on the sliding surface and do not involve the usual machine-sliding surface interactions or time-dependent friction seen in experiments under humid conditions [Dieterich, 1978, 1981]. Consistently it was found that the instabilities in the dry experiments could be stabilized if the driving velocity was decreased or if humid argon was admitted to the sample. Note that although the stress drops in Figure 9 are comparable to those in Figure 7, the displacements during unstable slip are much smaller in Figure 9. This difference arises because the apparatus was not servo-controlled for the test in Figure 7 and as a result had a much lower machine stiffness for that test.

#### SUMMARY AND DISCUSSION

The effects resulting from drying the sliding surfaces and conducting friction tests in a very dry environment are summarized as follows: First, the overall coefficient of friction is much higher with the dry experiments than for tests conduc-

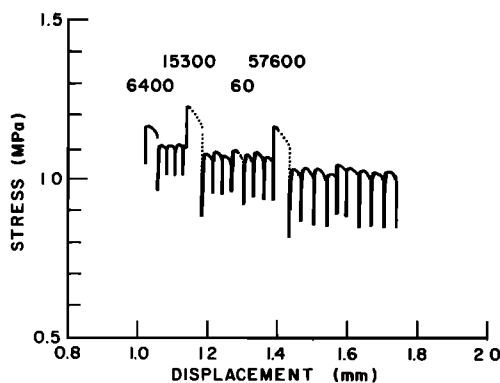


Fig. 7. Time-dependent test with sample of Eureka quartzite showing stick slip following reexposure to humid argon after drying. Loading velocity in this test was controlled by a manual needle valve, without use of servo-control. Numbers above the curve give hold time, in seconds, that the oil flow was shut off. Nominal loading rate between hold intervals is 1  $\mu\text{m/s}$ . Note that largest stick-slip stress drops follow each hold interval. Normal stress is 1.7 MPa.

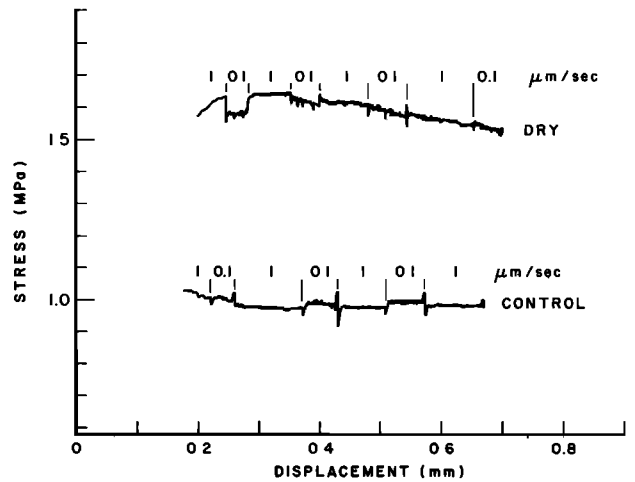


Fig. 8. Velocity stepping experiments for control experiment and dried samples in dry argon. Eureka quartzite at 1.7-MPa normal stress.

ted under humid conditions. Second, drying inhibits the time-dependent increases in the coefficient of friction of nominally stationary surfaces. Reexposure of the dried samples to a humid environment restores the time-dependent strengthening effect. Third, large stick-slip instability can be eliminated by drying and restored by reintroduction of humidity. Fourth, direct velocity dependence of friction is unaffected by drying, at least to the extent that an increase in sliding speed produces a comparable immediate increase in sliding friction under both dry and humid conditions. However, a competing inverse velocity dependence that becomes fully evident only after a finite displacement at a new velocity is strongly affected by drying. As a result, the dry surfaces yield a net increase in friction with increased slip speed, while the humid experiments usually produce a slight net decrease in friction with increased sliding speed. Fifth, an unusual, very small scale, velocity-controlled slip instability is observed only in some dry experiments.

Our interpretation of these results is made through reference to the processes outlined at the beginning of this paper that have been inferred to control the details of frictional slip under humid conditions.

Dried samples tested in a dry atmosphere yield a coefficient of friction that significantly exceeds the coefficient of friction for tests under humid conditions (Figure 4). That this strengthening effect originates because of drying is confirmed by the tests shown in Figure 5 in which the dry samples lose strength when exposed to humid argon after testing commenced. In the latter tests, frictional strength begins to decrease immediately following exposure to the humid atmosphere. In addition, the rate of strength loss appears to be controlled by the rate of diffusion of water onto the sliding surfaces. The sample which had grooves inscribed on the sliding surfaces to provide shorter diffusion paths along the surfaces display a more rapid decrease in strength than the ungrooved samples (Figure 5c). The strengthening effect of drying may originate from either or both of the following causes: (1) drying increases the efficiency of adhesion at points of contact by removing contaminate boundary layers that partially interfere with adhesion; (2) the drying process increases the strength of the substrate that supports the shear stress at points of contact (or increases the strength of interlocking

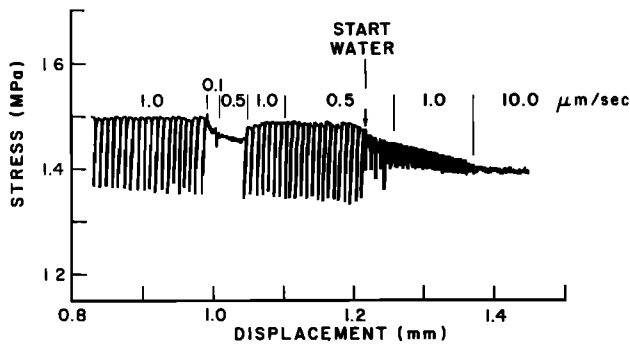


Fig. 9. Microinstabilities in initially dry servo-controlled tests with Eureka quartzite at 1.7-MPa normal stress. Average slip velocity in microns per second is indicated above the stress versus displacement curve.

asperities) making it more difficult to shear off surface irregularities. A third explanation, namely, that drying causes some type of mechanical change that leads to an increase in the real area of contact or increased penetration of asperities into opposing surfaces, is considered implausible because it would require that drying produces weaker surfaces which is contrary to the usual weakening effect of water.

The effect of drying in inhibiting time-dependent increases in friction (Figure 6) is well established by these experiments and confirms earlier predictions. This result appears to support definitively the conclusion that increase in friction with the logarithm of the time of contact is caused by water-assisted creep that increases the real area of contact. As noted above, this interpretation is supported by microindentation tests on a variety of nonmetallic solids that show analogous creep that increases the area of indenter contact with the logarithm of time.

We believe an important result of the experiments reported here is the documentation of the role of water in causing large-scale stick-slip instability. The consequences of time- and velocity-dependent friction and slip-induced changes in the population of contacts are outlined in earlier sections of this paper and have been previously explored in some detail utilizing constitutive models [Dieterich, 1978, 1979, 1981]. A major conclusion of those studies is that conventional large-scale stick-slip instability and, by analogy, earthquake instability on crustal faults originate because of the indentation creep effects. This study demonstrates that large-scale stick-slip instability along with time-dependent frictional changes could be eliminated by drying and restored by reexposure to moisture.

In addition to real area of contact, the other factor that directly determines frictional strength is the specific shear strength of the load-supporting contacts (i.e., the shear strength/unit area of real contact). It will be recalled that for a fixed area of contact, increases of velocity produce increases in strength. This effect is most evident from the jumps in frictional strength that result when sliding velocity is stepped to a new velocity (Figures 2 and 8). The constitutive models of Dieterich [1979, 1981] and Ruina [1983] indicate that velocity dependence of contact shear strength also causes the stress relaxation that occurs when the driving ram is held fixed and the surfaces continue to creep (Figures 1 and 4). The higher coefficient of friction obtained for the dry tests shows that the shear strength of the contacting asperities is strongly affected by humidity. However, in contrast to contact area creep, drying does not appear to eliminate the velocity dependence

of the contact shear strength. In the dry experiments the immediate changes in frictional resistance for a step change in velocity were comparable to the changes seen for humid tests, but at an overall higher level. We tentatively conclude therefore that drying simply acts to shift the velocity dependence to higher stresses. Similarly, relaxation creep during the hold intervals of the time-dependent tests was more evident in the dry than in the humid cases. We believe this greater creep in the dry case is not due to greater velocity dependence of contacts in shear, but is caused by elimination of the contact area creep effect which under humid conditions increasingly inhibits creep as the surfaces "heal" during the hold cycle.

We conclude that these experiments yield a consistent picture of the effects of water on the processes controlling friction. Drying increases the shear strength of points of contact but does not eliminate the velocity dependence of contact shear strength. However, drying does greatly reduce or eliminate the contact creep effect that under humid conditions tends to "heal" the surfaces by time-dependent increases in the true area of contact. Because drying more strongly reduces contact area creep than it does the competing velocity dependence of contact shear strength, the net change of friction for a change in sliding velocity can be of opposite signs for dry and humid conditions (Figure 8).

The specific mechanisms by which water accomplishes these effects is not evident from our experiments alone. Interactions at the scale of load-supporting contacts are complicated and potentially involve a number of water-assisted mechanisms. Surface properties and adsorbed species may greatly affect friction by interfering with adhesion of contacts [e.g., Bowden and Tabor, 1964]. Water significantly reduces the surface free energy of silicates [Parks, this issue] and is well known to result in large changes in fracture strength and crack propagation velocity [Freiman, this issue; Atkinson, this issue]. Adsorbed water and other mechanically active chemical species have been found to reduce near-surface indentation hardness of nonmetals through enhanced dislocation mobility [Westwood et al., 1967]. Finally, water enhances intracrystalline plasticity [Griggs and Blacic, 1965].

Although applied normal stress in these tests is very low, the normal stress at the actual points of contact between the sliding surfaces is probably very high. It is the central element of friction theory [Bowden and Tabor, 1964; Rabinowicz, 1965] that contact stresses are largely independent of normal stress and may approach the indentation strength of the material. For quartz, indentation strength is approximately 10 GPa [Brace, 1963; Scholz and Engelder, 1976], and direct measurements of real contact area in sliding friction experiments suggest contact normal stress may be somewhat lower (for example 1–2 GPa [Teufel and Logan, 1978]). At those high stresses, very localized water-assisted plastic flow and fracturing probably occur. Indentation creep studies cited above have shown that for some nonmetallic solids, indentation creep may involve plastic flow due to chemically enhanced dislocation mobility near to the surface. At room temperature in brittle silicates, it is plausible that water-aided time-dependent crack growth may aid or dominate the contact area creep effect.

The mechanisms of failure of load-supporting contacts due to shear displacement are poorly understood. The generation of abundant wear particles (fault gouge) and extensive surface damage confirms that the process is accompanied in part by crack propagation and brittle failure. In the tests reported here, the apparent dependence of shear strength on water and

the persistence of the velocity effect in dried samples are compatible with asperity failure by water-aided cracking. Experimental measurements of crack velocity and crack extension forces in glass and quartz [Freiman, this issue; Atkinson, this issue] demonstrate that the drying acts to increase the crack extension force required to propagate a crack at a given velocity. Velocity dependence of subcritical crack growth apparently persists, except under the very driest of conditions coupled with high crack propagation velocity.

An unexpected result from the dry tests is the occurrence of velocity-controlled small-scale instabilities (Figure 9). We believe these instabilities have an origin distinct from the usual large stick-slip instabilities encountered in friction tests under ambient laboratory humidity or water-saturated conditions. The instabilities that occur under the very dry conditions are of small amplitude and could not be stabilized by servo-controlling. These characteristics are indicative of rapid onset of unstable slip and interactions localized to the sliding surfaces. However, the instabilities could be stabilized by decreasing the driving speed or by reexposure of the samples to humidity. These features are distinct from time-dependent friction-controlled stick slip which is associated with contact area creep and which tends to be stabilized by increased driving speed and by drying. We surmise that the instabilities in the dry experiments originate because of unstable brittle failure of the load-supporting contacts in shear. Control of the instability by velocity and water are consistent with this explanation. At high velocities under dry conditions, crack propagation can become independent of velocity and hence intrinsically unstable. If the contacts accommodate slip by brittle failure, then unstable crack propagation may lead to local unstable slip. At slower velocities or by adding humidity, crack propagation becomes velocity dependent, and hence brittle failure of load-supporting asperities is locally stable.

*Acknowledgments.* We wish to thank Tracy Johnson, Steve Kirby, and John Logan for thoughtful reviews that lead to several improvements in this paper.

#### REFERENCES

- Atkinson, B. K., Subcritical crack growth in geological materials, *J. Geophys. Res.*, this issue.
- Bowden, F. B., and D. Tabor, *The Friction and Lubrication Solids*, vol. 2, Clarendon, Oxford, 1964.
- Brace, W. F., Behavior of quartz during indentation, *J. Geol.*, 71, 581-595, 1963.
- Dieterich, J. H., Time-dependent friction in rocks, *J. Geophys. Res.*, 77, 3690-3697, 1972.
- Dieterich, J. H., Time-dependent friction and mechanics of stick-slip, *Pure Appl. Geophys.*, 117, 790-806, 1978.
- Dieterich, J. H., Modelling of rock friction, 1, Experimental results and constitutive equations, *J. Geophys. Res.*, 84, 2161-2168, 1979.
- Dieterich, J. H., Constitutive properties of faults with simulated gouge, in *Mechanical Behavior of Crustal Rocks*, *Geophys. Monogr. Ser.*, vol. 24, pp. 103-120, AGU, Washington, D. C., 1981.
- Evans, B., and C. Goetze, The temperature variation of hardness of olivine and its implication for polycrystalline yield stress, *J. Geophys. Res.*, 84, 5505-5524, 1979.
- Freiman, S. W., Effects of chemical environments on slow crack growth in glasses and ceramics, *J. Geophys. Res.*, this issue.
- Griggs, D. T., and J. D. Blacic, Quartz-anomalous weakness of synthetic crystals, *Science*, 147, 292-295, 1965.
- Higgs, N. G., and J. M. Logan, Frictional properties of ultrafine quartz in upper-crustal earthquake environments (abstract), *Eos Trans. AGU*, 61, 1037, 1981.
- Parks, G. A., Surface and interfacial free energies of quartz, *J. Geophys. Res.*, this issue.
- Rabinowicz, E., *Friction and Wear of Materials*, John Wiley, New York, 1965.
- Ruina, A. L., Slip instabilities and state variable friction laws, *J. Geophys. Res.*, 88, 10,359-10,370, 1983.
- Scholz, C. H., and J. T. Engelder, The role of asperity indentation and ploughing in rock friction, I, Asperity creep and stick-slip, *Int. J. Rock Mech. Min. Sci. Geomech. Abstr.*, 13, 149-154, 1976.
- Scholz, C. H., P. Molnar, and T. Johnson, Detailed studies of frictional sliding of granite and implications for the earthquake mechanism, *J. Geophys. Res.*, 77, 6392-6406, 1972.
- Teufel, L. W., and J. M. Logan, Effect of shortening rate on the real area of contact and temperatures generated during frictional sliding, *Pure Appl. Geophys.*, 116, 840-865, 1978.
- Walker, W. W., and L. J. Demer, Effects of loading duration on indentation hardness, *Trans. Am. Inst. Min. Metall. Pet. Eng.*, 230, 613-614, 1964.
- Westbrook, J. H., and P. J. Jorgensen, Indentation creep of solias, *Trans. Am. Inst. Min. Metall. Pet. Eng.*, 233, 425-428, 1965.
- Westbrook, J. H., and P. J. Jorgensen, Effects of water desorption on indentation microhardness anisotropy in minerals, *Am. Mineral.*, 53, 1899, 1968.
- Westwood, A. R. C., D. L. Goldheim, and R. G. Lye, Rebinder effects in MgO, *Philos. Mag.*, 16, 505-519, 1967.

G. Conrad and J. H. Dieterich, U.S. Geological Survey, 345 Middlefield Road, Mail Stop 77, Menlo Park, CA 94025.

(Received May 2, 1983;  
revised October 7, 1983;  
accepted October 10, 1983.)